Supporting Information

The Nanostructured Poly(L-lactic acid)-Poly(ethylene glycol)-Poly(L-lactic acid) Triblock Copolymers and their CO_2/O_2 Permselectivity

Yun Xueyan[a], Li Xiao fang[a], Pan Pengju[b], Dong Tungalag[a,*]

a. College of Food Science and Engineering, Inner Mongolia Agricultural University, 306 Zhaowuda Road. Hohhot, Inner Mongolia, China, 010018. E-mail: dongtlg@163.com

b. College of Chemical and Biological Engineering, Zhejiang University, 38 Zheda Road, Hangzhou 310027, China.

Supporting Information

NMR spectroscopy, differential scanning calorimetry, Fourier transform infrared spectrum, X-ray scattering, CO_2 and O_2 permeability, water vapor permeability (of all copolymers except as mentioned in the main text)

EXPERIMENTAL

Differential Scanning Calorimetry (DSC)

The isothermal crystallization and subsequent melting behavior of PLGL triblock copolymers as well as the neat PLLA were measured with differential scanning calorimetry (DSC Q20, TA Instruments, Co., USA) under a nitrogen purge. Each sample was weighed approximately 5 ~ 10 mg and encapsulated in an aluminum pan. Two different DSC heating process were used: First, the samples were initially scanned from 25 to 200ºC with a heating rate of 10ºC/min; Second, the samples were initially scanned from 25 to -50ºC and then heating to 200ºC with a heating rate of 10 ºC/min. Thermal parameters including T_g, melting temperature (T_m), cold crystallization temperature (T_{cc}) and crystallization temperature (T_c) can be obtain from the thermal curves. The cold crystallization enthalpy (ΔH_{cc}), crystallization enthalpy (ΔH_c) and melting enthalpy (ΔH_m) are calculated from the DSC curves when the samples were initially scanned from 25 to 200ºC. The degree of crystallinity (X_c) was calculated from Eq.(1), ΔH_o is the enthalpy of polymers film with 100% crystallinity (PLLA: ΔH_o = 93 J/g; PEG: ΔH_o = 208 J/g) [1,2].

$$X_c = \frac{\Delta H_m - \Delta H_{cc}}{\Delta H_o} \qquad (1)$$

Scanning Electron Microscopy (SEM)

A scanning electron microscope (TM4000Plus, HITACHI, Japan) with an accelerating voltage of 10 kV was used to evaluate the morphology of film's surface. The samples were sputter-coated with gold particles before the surface characterization.

RESULTS AND DISCUSSION

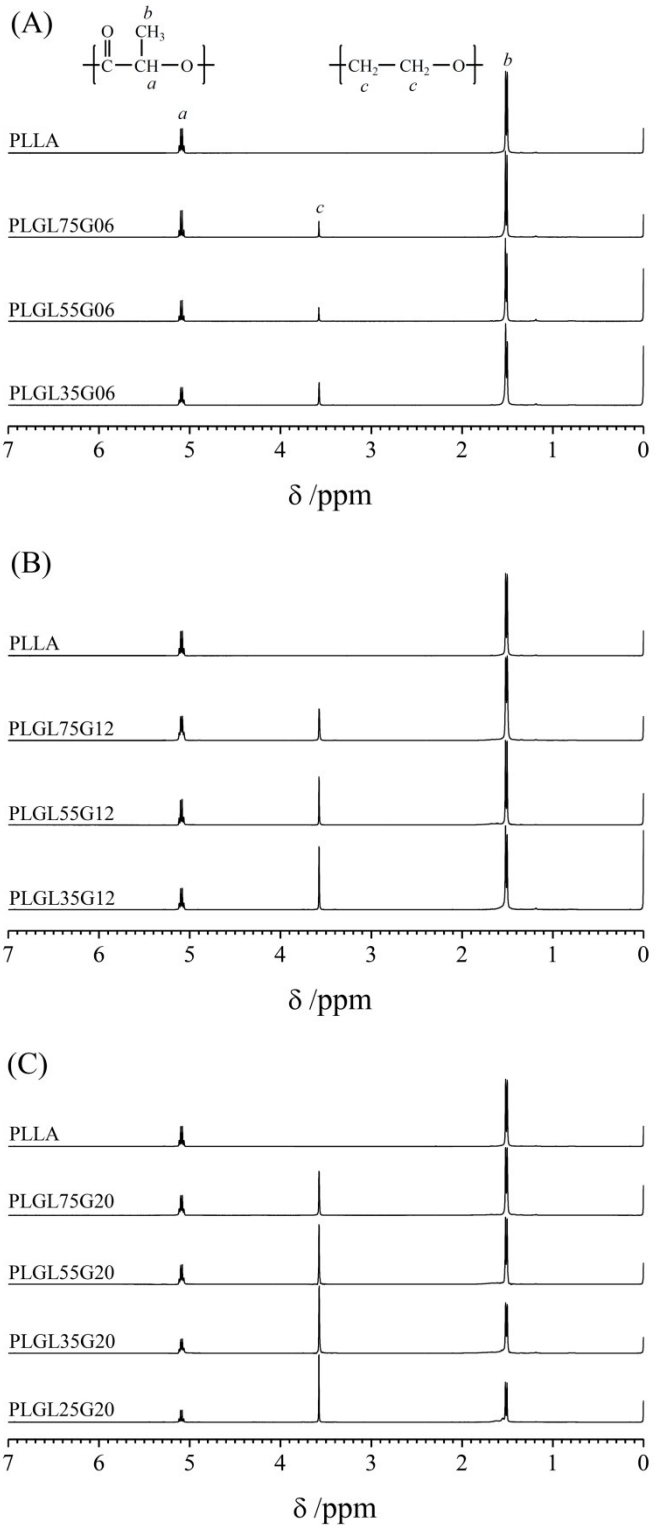

Figure S1 ^{1}H NMR spectra of the PLLA and copolymers

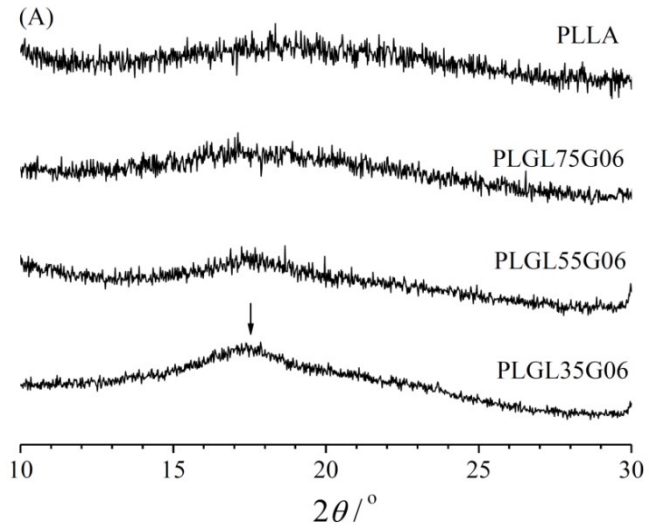
(A)
PLLA
PLGL75G06
PLGL55G06
PLGL35G06
10
15
20
25
30
2θ/°

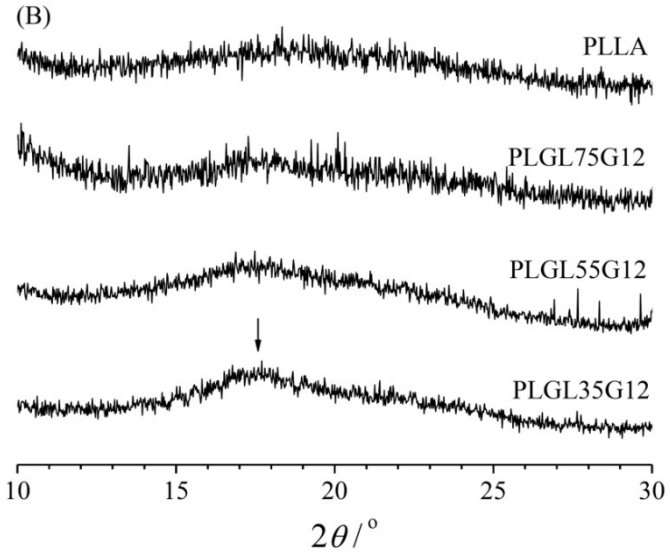
(B)
PLLA
PLGL75G12
PLGL55G12
PLGL35G12
10
15
20
25
30
2θ/°

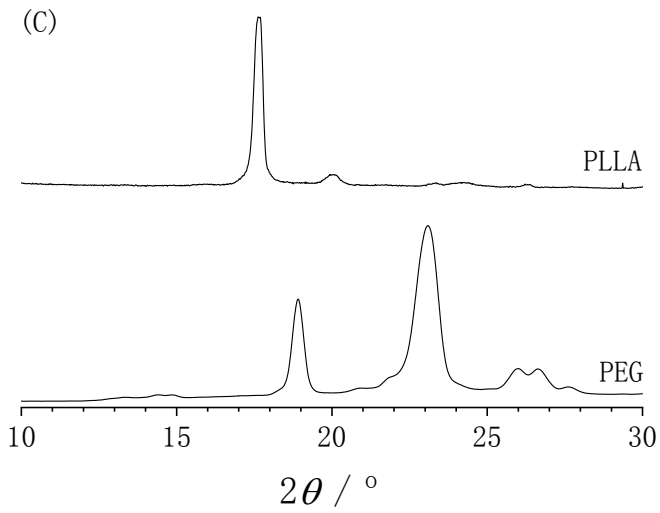

Figure S2 The WAXD pattern of PLLA, PEG, PLGLxG06 and PLGLxG12 copolymers

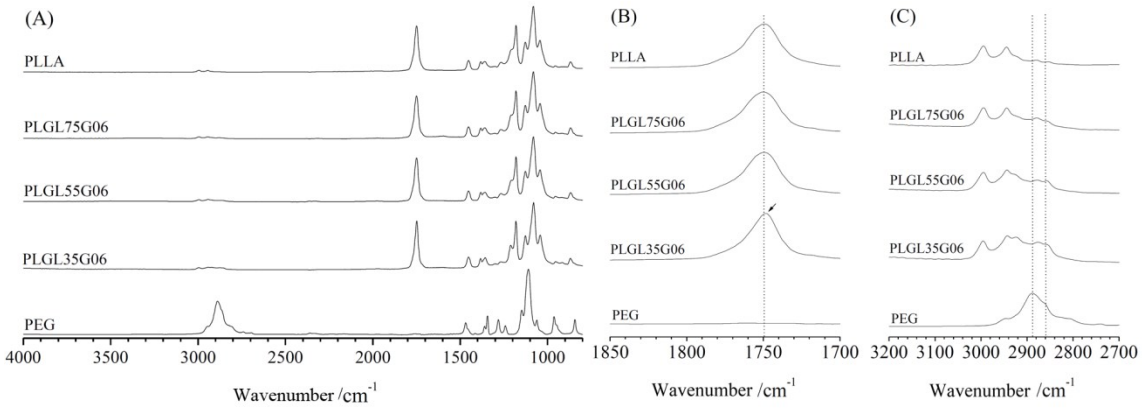

Figure S3 The FTIR spectra of PLLA, PEG and PLGLxG06 copolymers

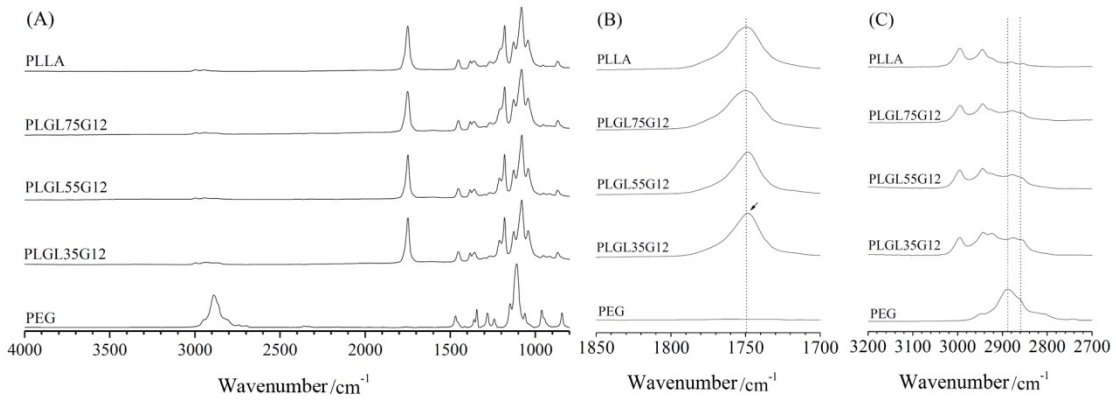

Figure S4 The FTIR spectra of PLLA, PEG and PLGLxG12 copolymers

DSC Results Analysis

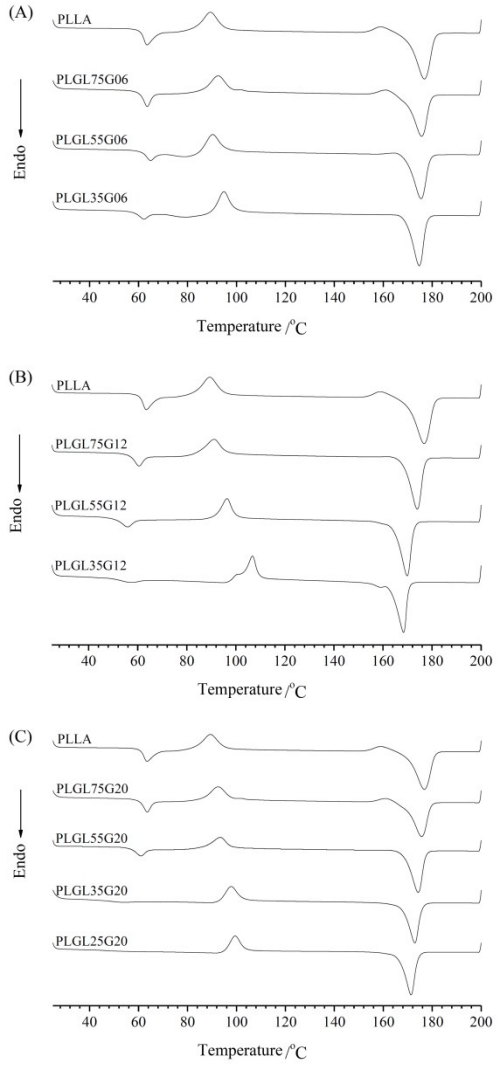

Figure S5 the DSC traces of PLLA and PLGLxGy triblock copolymers with various PEG contents recorded during the first heating scan from 25 to 200°C

Table S1 The thermal characteristics of PLLA and PLGLxGy triblock copolymers

Sample	PEG block			PLLA block					
	$T_m^{(a)}$ /°C	$\Delta H_m^{(a)}$ /J·g^{-1}	X_c /%	$T_g^{(a)}$ /°C	$T_{cc}^{(a)}$ /°C	$\Delta H_{cc}^{(a)}$ /J·g^{-1}	$T_m^{(a)}$ /°C	$\Delta H_m^{(a)}$ /J·g^{-1}	X_c /%
PLLA	-	-	-	61.2	89.4	45.8	176.8	48.9	3.3
PLGL75G06	-	-	-	61.1	92.6	44.3	175.7	46.2	2.0
PLGL55G06	-	-	-	62.7	90.3	39.9	175.5	41.3	1.5
PLGL35G06	-	-	-	60.4	94.9	42.9	174.7	48.0	5.4
PLGL75G12	-	-	-	57.8	91.2	42.5	173.8	45.8	3.5
PLGL55G12	-	-	-	53.3	99.4	43.1	170.3	49.4	6.8
PLGL35G12	-	-	-	53.5	107.0	40.3	168.2	48.7	8.9
PLGL75G20	-	-	-	60.9	92.6	46.4	175.7	47.3	1.0
PLGL55G20	-	-	-	58.6	93.5	39.2	174.3	49.5	11.1
PLGL35G20	-	-	-	45.2	97.8	39.4	172.9	50.1	11.5
PLGL25G20	-	-	-	46.0	99.5	40.7	171.7	51.5	11.7

Note：(a) Determined by DSC heating scan(25 →200 °C)；ΔH_m and ΔH_{cc} were normalized with weight percentage of PLLA (or PEG).

Figure S5 showed the DSC traces of PLLA and PLGLxGy triblock copolymers with various PEG contents recorded during the first heating scan from 25 to 200°C and the thermal characteristics obtained from the curves are summarized in Table S1. It can be seen that the thermal property of copolymers was strongly depend on the variation of composition of PLLA and PEG. The T_m of pure PLLA was about 176.8°C and the T_g was about 61.2°C. The cold crystallization peak and recrystallization peak of PLLA can be observed at 89.4 and 160°C, respectively. For copolymers with certain molecular weight PEG, the PEG level has relative increased with the decrease of the PLLA chains (Table S1). The T_m and T_g of PLLA in copolymers shift to lower temperature.

Furthermore, it can be seen form figure S5 (A) and table S1, for PLGLxG06 copolymers, the T_m of PLLA only slightly decreased from 176.8 to 174.7°C. The changes of the T_{cc} and T_g of PLLA were also minor. This is because few PEG with small molecular weight doesn't have a very good plasticizing effect.

As the molecular weight of PEG further increased to 12000, it can be seen from

S5(B) and table S1 that the T_m of PLLA shifts from 176.8°C to 168.2°C. Meanwhile, the T_g shifts from 61.2°C to 53.3°C. It noteworthy that the T_{cc} of PLGLxG12 copolymers increased with the increase of PEG content. The T_{cc} of PLGL3G12 reached 107.0°C, which 20°C higher than pure PLLA.

For PLGLxG20 copolymers, the content of PEG increased to over 15% (Table 1), the T_g further decreased and the T_{cc} kept increased. The T_g of PLGL25G20 was about 46.0°C and the T_{cc} increased to 99.5°C, indicating that the addition of PEG improved the mobility and flexibility of PLLA . Besides, it also can be seen from figure S5 (B) and (C) that the recrystallization peak become smaller with the increase of PEG content.

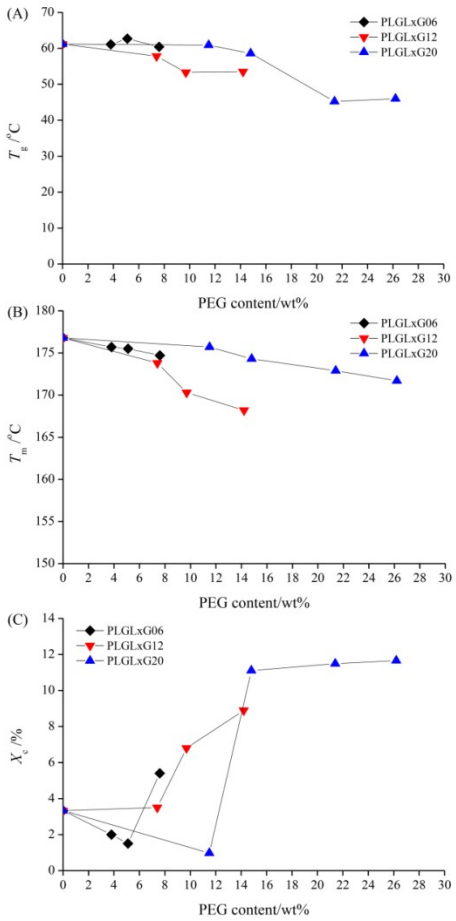

Figure S6 the changes of T_g, T_m and X_c of copolymers with the increase of the PEG content during the first heating scan from 25 to 200°C

Figure S6 summarized the changes of T_g, T_m and X_c of copolymers with the increase of the PEG content during the first heating scan from 25 to 200°C. It can be seen from figure S6(A) and (B) that the T_g and T_m of PLGLxGy copolymers decreased with the increase of PEG content. It noteworthy that T_g and T_m of PLGLxG12 decrease more rapidly than the other copolymers. However, the T_g and T_m of PLGLxG20 began decreased rapidly when the content of PEG higher than 18%.

As shown in figure S6(C), the X_c increased with the increase of PEG in PLGLxG12 copolymers. For PLGLxG06 and PLGLxG20 copolymers, the X_c firstly decreased slightly and then increased with the increase of PEG content, Finally, all PLGLxGy copolymers exhibit a higher X_c value than pure PLLA. This phenomenon indicated that PLLA and few PEG with low molecular weight were partly compatible and prevent the crystallization of PLLA. As the increase of molecular weight and content of PEG, both the PEG and PLLA chains can gathered and part of the PLLA can crystallize easily. Aggregation of the two different phases can easily lead microphase separation. This is well according the AFM and TEM results.

During the first heating scanning, no obvious peaks were observed for PEG, indicating an amorphous state of PEG. To further investigate the crystalline state of PEG blocks in copolymers, the sample was cooling from 200 to -50°C. Figure S7 depicts the cooling curves from 200 to -50°C. As shown in figure S7(A) and (B), there still no peaks related to PEG appeared and only crystallization peaks of PLLA were observed at 100°C in DSC cooling curves of PLGLxG06 and PLGLxG12.

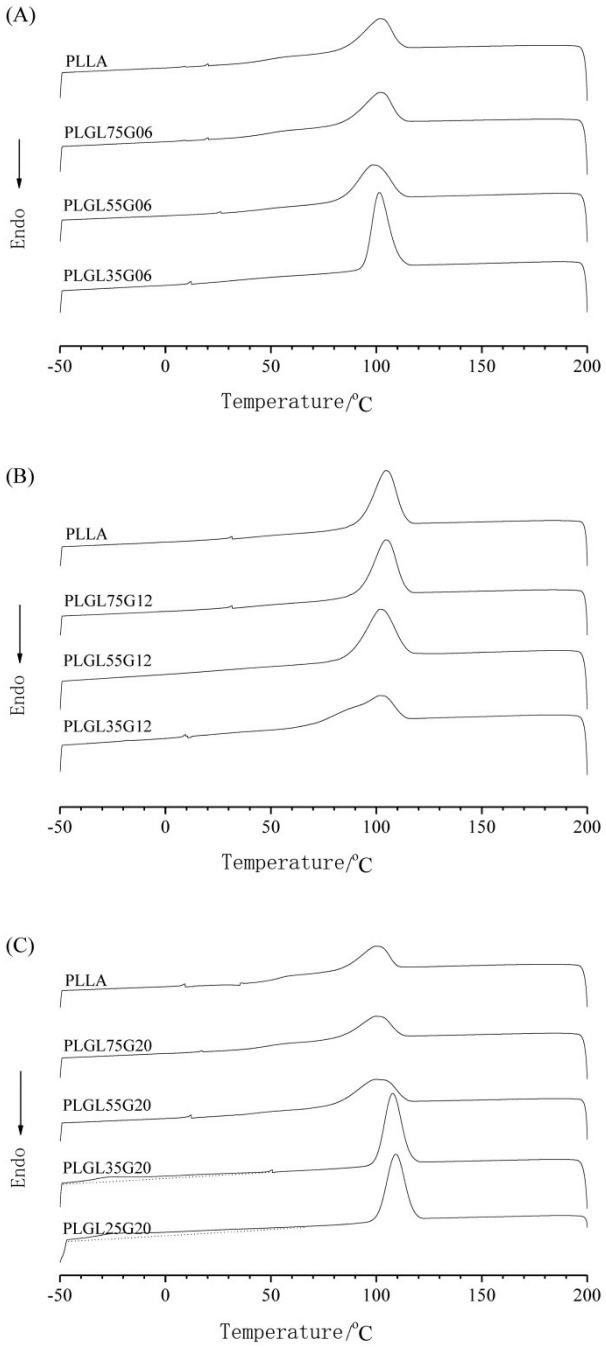

Figure S7 the cooling curves of PLLA and copolymers from 200 to -50°C

Nevertheless, a crystallization peak attributed to PEG appeared at -30°C in enlarged curves of PLG75G20 and PLG55G20. With the content of PEG further increasing, small crystallization peaks of PEG can be directly observed in DSC curves of PLGL35G20 and PLGL25G20. The T_m, T_g, and X_c of PEG blocks during the cooling process are listed in Table S2. It can be seen that the T_g of PLLA shifts to

lower temperature with the increase of the PEG content. However, the X_c of PLLA increased with the increase of the molecular weight and content of PEG. This indicated that the flexible PEG block enhanced the mobility of PLLA chains and PLLA was crystallized more easily during the cooling process.

Table S2 The thermal characteristics of PLLA and PLGLxGy triblock copolymers

	PLLA block							
Sample	$T_c^{(a)}$ /°C	$\Delta H_c^{(a)}$ /J·g^{-1}	$T_g^{(b)}$ /°C	$T_{cc}^{(b)}$ /°C	$\Delta H_{cc}^{(b)}$ /J·g^{-1}	$T_m^{(b)}$ /°C	$\Delta H_m^{(b)}$ /J·g^{-1}	X_c /%
PLLA	99.5	18.4	56.7	102	21.7	174.9	49.3	29.7
PLGL75G06	99.7	20.1	53	99.4	15.5	175.7	46.6	33.3
PLGL55G06	98.1	29.8	50.7	92.4	3.4	175.3	46.2	45.7
PLGL35G06	101.3	38.3	41.8	-	-	74.7	43.9	46.9
PLGL75G12	104.3	37.7	44.7	-	-	174	48.2	51.5
PLGL55G12	100.1	41.8	-	-	-	170.1	54.6	58.4
PLGL35G12	101.4	28.8	36.7	77.8	5.2	167.4	53.2	51.3
PLGL75G20	99.7	23.8	53.2	99.4	16.2	175.6	48.7	35.0
PLGL55G20	99.4	31.6	46.8	90.8	8.0	174.3	51.6	46.9
PLGL35G20	107.7	45.4	31.3	-	-	172.6	51.5	55.4
PLGL25G20	106.8	47.2	-	-	-	171.1	54.5	58.6
	PEG block							
Sample	$T_c^{(a)}$ /°C	$\Delta H_c^{(a)}$ /J·g^{-1}	$T_g^{(b)}$ /°C	$T_{cc}^{(b)}$ /°C	$\Delta H_{cc}^{(b)}$ /J·g^{-1}	$T_m^{(b)}$ /°C	$\Delta H_m^{(b)}$ /J·g^{-1}	X_c /%
PLLA	-	-				-	-	-
PLGL75G06	-	-				-	-	-
PLGL55G06	-	-				-	-	-
PLGL35G06	-	-				-	-	-
PLGL75G12	-	-				-	-	-
PLGL55G12	-	-				-	-	-
PLGL35G12	-	-				-	-	-
PLGL75G20	-14.7	1.0				-	-	-
PLGL55G20	-20.3	7.6				-	-	-
PLGL35G20	-26.8	24.8				39.7	35.0	16.8
PLGL25G20	-25.9	32.8				38.9	38.9	18.7

Note：(a) Determined by DSC heating scan (200→-50 °C); (b) Determined by DSC heating scan (-50 →200ºC);Δ*H*m and Δ*H*cc were normalized with weight percentage of PLLA (or PEG).

For PEG blocks in copolymers, the few PEG with low molecular weight has good compatibility with PLLA . In this situation, PEG was totally amorphous. In

PLGLxG20 copolymers, board crystallization peaks can be observed in range of -15-27 °C after enlarging the DSC curves. Furthermore, the T_c decreased with the increase of PEG content. The X_c of PEG was 16.8% in PLGL35G20 copolymers. Those crystallized PEG was melting at 40°C in the second heating curves(Figure S8). This result indicated that most of the original PEG in copolymers was in amorphous state and partly crystallized during cooling process.

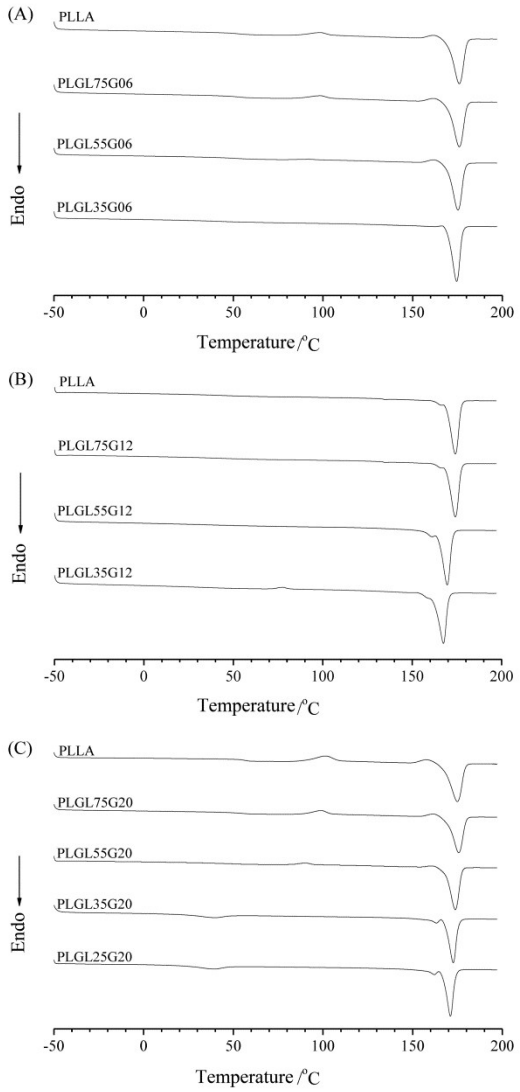

Figure S8 the second heating scanning DSC curves of PLLA and PLGLxGy copolymers

The samples were then second heated from -50 to 200°C at 10°C·min^{-1}. Figure

S8 presents the second heating scanning DSC curves of PLLA and PLGLxGy copolymers. Since PEG was totally in amorphous state in PLGLxG06 and PLGLxG12 copolymers, only melting peak of PLLA was observed at 170°C in DSC heating curves. For PLGLxG20 copolymers, no obvious melting peaks of PEG in PLG75G20 and PLG55G20. With the PEG content further increase, a small melting peak at 40°C in PLGL35G20 and PLGL25G20 copolymers. Those small melting peaks were due to few crystallized PEG in the cooling process. In other words, most PEG were in amorphous state in copolymers. Besides, a small crystallization peak appeared at 80~100°C, which due to un-fully crystallized PLLA during the cooling process.

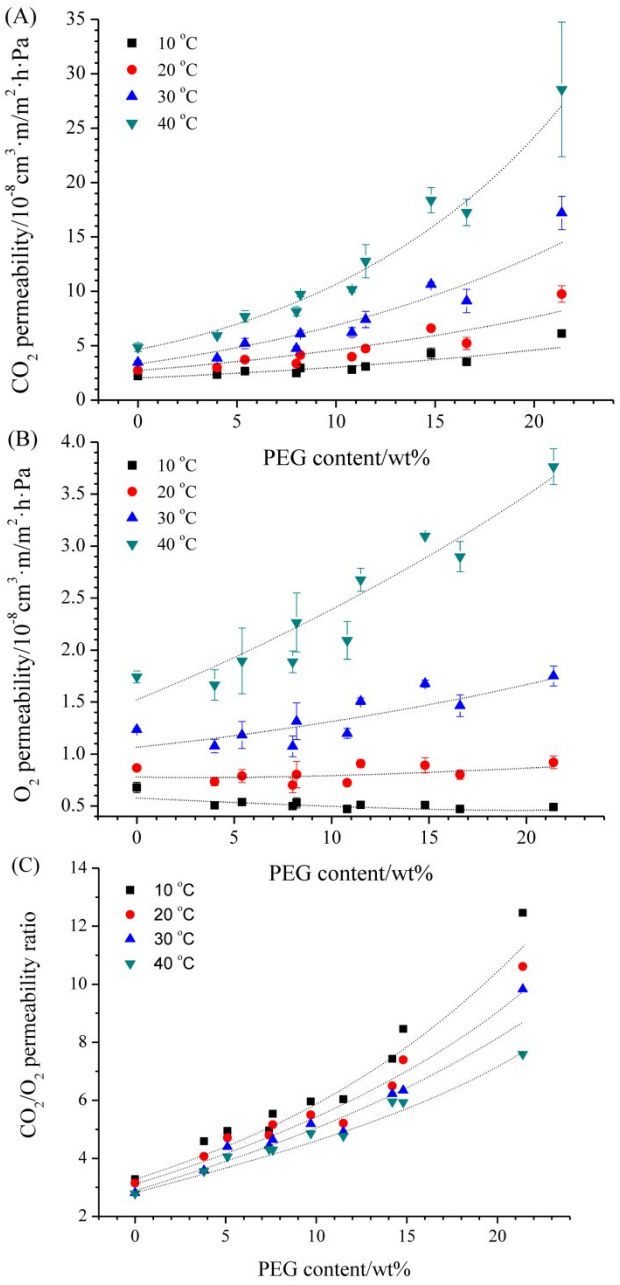

Figure S9 the variation of CP, OP and $P_{C/O}$ with PEG content in copolymers

Figure S9 shows the variation of CP, OP and $P_{C/O}$ with PEG content in copolymers. It can be seen that the PEG content has a minimal impact on the CP of the copolymers, and the CP values increased fairly slowly with an increase of PEG content below 30°C. However, the CP values were significantly influenced by increasing PEG content as the temperature increased. The CP values of copolymers below 40°C were obviously higher than the CPs at lower temperatures. The more

PEG, the lower the T_g of the copolymers. When the temperature was close to the T_g of the copolymers, the mobility of polymer chains increased. In addition, heating a gas causes the molecules to move faster. Apart from the above two factors, the main reason is that PEG has strong preferential adsorption and diffusion for CO_2, and this permeability plays a key role at high temperatures than it does with the others. Thus, the CP increased with increasing PEG content at higher temperatures.

As seen from figure S9(B), the oxygen permeability of the copolymers differed greatly in the way they change with CO_2 permeability at relative higher temperatures. At 10 and 20°C, the OPs of copolymers decreased with increasing PEG content. However, the OP values increase slowly with increasing PEG as the temperature is increased further to 30 and 40°C. Possible explanations for this phenomenon are as follows:

(1) As shown in Figure 3, the AFM images for PLLA and PLGLxG20 copolymers indicate that a small amount of PEG can disperse uniformly in PLLA and were compatible with PLLA blocks in the copolymers. A small amount of PEG dispersed throughout the amorphous regions of the PLLA blocks, leading to a decrease of free volume between the amorphous PLLA chains. Thus, it becomes very difficult for gas molecules to permeate the film, leading to a decrease of OP in a low temperature environment.

(2) However, the PEG has a quite low melting point of approximately 60°C,[3] and the PEG block produces good mobility at higher temperature, leading to a lower T_g, and to better mobility of the copolymer with more PEG at higher temperatures. Thus, the free volume between chains with more PEG or at higher temperatures was also increased. This is the reason the OP values increased with an increase of PEG at higher temperatures.

Figure S9(C) presents the change of CO_2/O_2 permselectivity of copolymer films with variation of PEG content at different temperatures. Based on these results, the $P_{C/O}$ values increased slowly with increasing PEG content. However, it should be noted that the higher the temperature, the slower the rate of increase of the $P_{C/O}$. Thus, all copolymers have higher $P_{C/O}$ values at lower temperatures. Considering both Figures S10(A) and S10(B), this is due to the different ways the OP and CP changed with PEG content at different temperatures.

SEM micrographs of film's surface

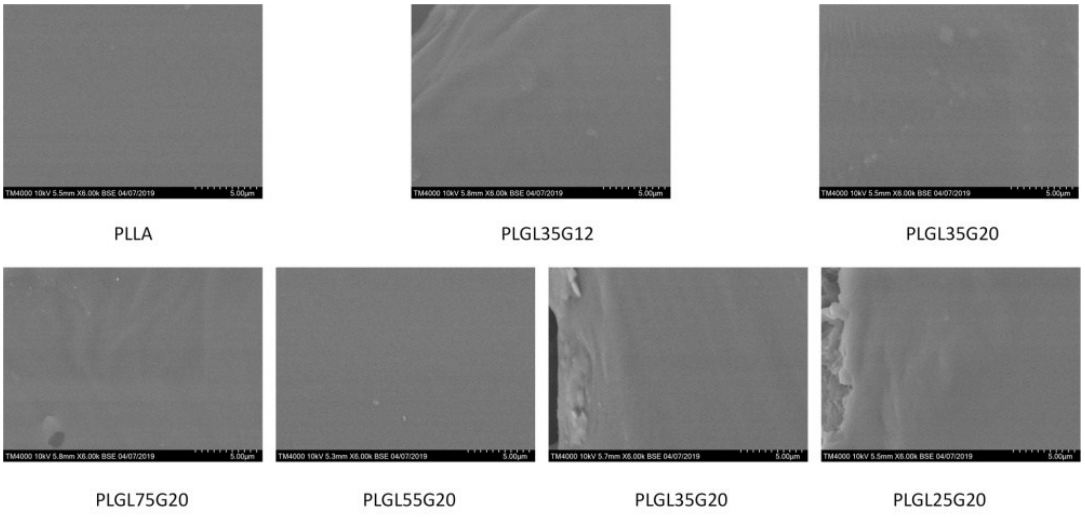

Figure S10 the SEM micrographs of PLLA and PLGLxGy copolymers

The SEM micrographs can further reveal the surface characteristics of samples. Figure S10 shows the SEM result of films. As shown in Figure S10, only smooth and homogeneous surfaces were observed in most micrographs. It should be notice that the different morphology appeared at the edge of PLGL35G12, PLGL35G20 and PLGL25G20 were attribute to the fracture surface at the end of the sample. The SEM micrographs indicated that the PLGLxGy copolymers films were free of obvious and visible porosity on their surface. Considering both SEM and AFM result (Figure 3),

the nanoscale microphase separation occurred in those copolymers and improve the gas permeability of films.

References

1. Dong T., Yu Z., Wu J., Zhao Z., Yun X., Wang Y., Jin Y. and Yang J., Polym. Sci. 2015, **57**, 738.

2. Dong T., He Y., Zhu B., Kyungmoo Shin A. and Inoue Y., Macromolecules, 2005, **38**, 7736.

3. Li, N., Xiao, C., Zhang, Z. Effect of polyethylene glycol on the performance of ultrahigh‐molecular‐weight polyethylene membranes. Journal of Applied Polymer Science, 2010, **117**, 720-728.

ACKNOWLEDGMENTS

The authors thank the National Natural Science Foundation of China (NO. 21564012), Double First-class Disciplines Innovation Team Building and Talent Cultivation Project of Inner Mongolia Agriculture University (2018) and The Scrolling Support of Prairie Talents Project (2017).